J. Fluid Mech. (2020), *vol.* 884, R1, doi:10.1017/jfm.2019.954

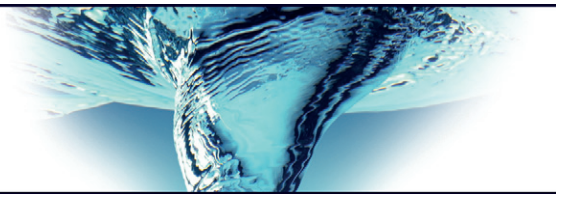

JFM RAPIDS
journals.cambridge.org/rapids

Self-organization of multiple self-propelling flapping foils: energy saving and increased speed

Xingjian Lin[2,3], Jie Wu[1,2,3,†], Tongwei Zhang[2,3] and Liming Yang[4]

[1]State Key Laboratory of Mechanics and Control of Mechanical Structures, Nanjing University of Aeronautics and Astronautics, Yudao Street 29, Nanjing, Jiangsu 210016, China

[2]Department of Aerodynamics, Nanjing University of Aeronautics and Astronautics, Yudao Street 29, Nanjing, Jiangsu 210016, China

[3]Key Laboratory of Unsteady Aerodynamics and Flow Control, Ministry of Industry and Information Technology, Nanjing University of Aeronautics and Astronautics, Yudao Street 29, Nanjing, Jiangsu 210016, China

[4]Department of Mechanical Engineering, National University of Singapore, 10 Kent Ridge Crescent, Singapore 119260, Singapore

(Received 13 July 2019; revised 14 October 2019; accepted 13 November 2019)

The collective hydrodynamics in fish schools and bird flocks, which includes self-organization of multiple dynamic bodies, is complex and lacks sufficient exploration. In this paper, we study the performance of multiple self-propelled foils in tandem formation, whose flapping motions are asynchronous with a phase difference. It is shown that a compact formation, in which all of the foils perform like a complete anguilliform swimmer, can be spontaneously formed by multiple foils via hydrodynamic interactions. Both velocity enhancement and energy saving can be achieved by multiple foils in anguilliform-like swimming. Furthermore, such anguilliform-like swimming behaviour can be observed over a wide range of parameters, including the number of foils, the phase difference, the initial distance, the heaving amplitude and the pitching amplitude. The results obtained here may provide some light on understanding the self-organization behaviour of biological collectives.

Key words: swimming/flying, vortex dynamics, vortex streets

1. Introduction

Self-organized collective motion of multiple moving bodies in fluids is ubiquitous in nature, including bacterial colonies (Koch & Subramanian 2011), sedimenting particles

† Email address for correspondence: wuj@nuaa.edu.cn

(Guazzelli & Hinch 2011) and animal groups (Couzin 2009). Amongst them, fish schools and bird flocks, as typical examples of biological collectives which can be easily observed, have received considerable attention from biologists, physicists and engineers for several decades (Hemelrijk & Hildenbrandt 2012). Why do they travel in groups? Some social traits have been proposed to explain their collective behaviours, such as for the purpose of foraging and protection from predators (Sumpter 2006). However, from the fluid mechanics perspective, it has been claimed that hydrodynamic interactions are crucial for the collective behaviours of fish schools and bird flocks (Becker *et al.* 2015; Filella *et al.* 2018).

The most quoted hydrodynamic function for fish schools and bird flocks is to reduce energy consumption (Portugal *et al.* 2014; Ashraf *et al.* 2017). However, the collective formations are different from each other in these theoretical and experimental studies, in which the hydrodynamic function of saving energy has been verified (Weihs 1973; Marras *et al.* 2015; Ashraf *et al.* 2017). On the other hand, evidence against the hydrodynamic advantage has been observed in some experiments with living fish schools and bird flocks (Partridge & Pitcher 1979; Usherwood *et al.* 2011). Consequently, the hydrodynamic function for fish schools and bird flocks is still controversial so far. For experiments with living fish schools and bird flocks, one of the primary challenges is that hydrodynamic interactions between individuals are hard to measure.

An effective strategy for investigating the hydrodynamics in fish schools and bird flocks is to use multiple flapping foils or hydrofoils in regular arrangements, in which both force and flow can be precisely measured (Dong & Lu 2007; Kurt & Moored 2018). By using this approach, some fundamental mechanisms underlying the performance of multiple dynamic bodies in regular formations have been revealed (Uddin, Huang & Sung 2015; Maertens, Gao & Triantafyllou 2017; Gao & Triantafyllou 2018). It has been indicated that hydrodynamic interactions can generate both constructive and destructive effects on the performance of individuals; which kind of hydrodynamic effect occurs depends on the regular arrangements (Kim, Huang & Sung 2010; Shoele & Zhu 2015; Muscutt, Weymouth & Ganapathisubramani 2017). For the tandem arrangement, when the separation distance is smaller than half of the chord length, the performance of each body varies significantly as compared with that of an isolated body (Boschitsch, Dewey & Smits 2014; Kurt & Moored 2018). When anti-phase motion is used, the thrust of the leader is increased, but that of the follower is decreased (Boschitsch *et al.* 2014). In addition, the opposite trends can be observed when in-phase motion is used (Boschitsch *et al.* 2014). Moreover, when the separation distance is approximately one chord length, performance variation can be observed only for the follower (Akhtar *et al.* 2004; Rival, Hass & Tropea 2011; Broering, Lian & Henshaw 2012). However, the individuals were fixed in the oncoming flow; namely, self-organization according to the hydrodynamic interaction is neglected in the previous work.

Recently, a self-propelled model consisting of two flapping foils, in which self-organization is considered, has been used for the investigation of fish schools and bird flocks (Peng, Huang & Lu 2018*a*). It has been indicated that flow-mediated interactions are crucial for the emergence of collective locomotion (Becker *et al.* 2015; Ramananarivo *et al.* 2016; Newbolt, Zhang & Ristroph 2019). For two identical bodies in tandem formation, two types of orderly formation – i.e. compact and sparse formations – can be self-organized via the hydrodynamic interactions (Zhu, He & Zhang 2014; Ramananarivo *et al.* 2016; Newbolt *et al.* 2019). Of particular interest is the compact formation, in which both foils are close to each other (the horizontal gap

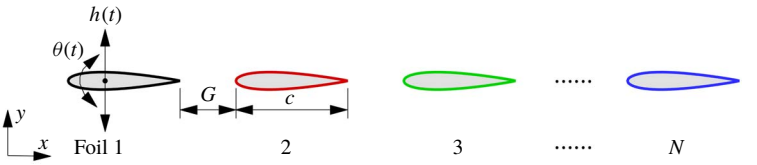

FIGURE 1. Sketch view of the simulation model. Here $h(t)$ and $\theta(t)$ respectively represent the heaving and pitching motions, G is the horizontal separation gap between two foils and c is the chord length.

is smaller than one chord length) and swim faster than the isolated foil (Zhu *et al.* 2014; Ramananarivo *et al.* 2016), although more energy is consumed (Zhu *et al.* 2014). Recently, considering the phase difference which can be generally observed in fish schools and bird flocks (Portugal *et al.* 2014; Ashraf *et al.* 2016), it has been revealed that both velocity enhancement and energy saving can be achieved by two asynchronous bodies in the compact formation (Lin *et al.* 2019*b*). However, only two bodies are considered in these previous studies, so the question of whether the compact formation could be achieved by multiple bodies together with velocity enhancement and energy saving is still an open question. Peng, Huang & Lu (2018*b*) indicated that the compact formation was only observed for few bodies (such as three bodies in their work), or else the compact formation would split into several subgroups when the number of bodies increased. However, the phase difference has never been considered for the hydrodynamic schooling of multiple dynamic bodies (Peng *et al.* 2018*b*; Lin *et al.* 2019*b*). The collective hydrodynamics of multiple asynchronous bodies is much more complex and still lacks sufficient exploration.

In this study, the performance of multiple tandem self-propelled foils, whose flapping motions are asynchronous with a phase difference, is numerically investigated. The specific aim here is to demonstrate that the compact formation can be self-organized by multiple asynchronous foils via flow-mediated interactions and that velocity enhancement and energy saving can be achieved by individuals in the compact formation. The remainder of this paper is organized as follows. The problem description and methodology are presented in § 2. The simulation results are addressed in detail with discussions in § 3. Finally, some conclusions are drawn in § 4.

2. Problem description and methodology

A self-propelled system consisting of multiple asynchronous flapping foils in tandem formation is proposed in the present study, as shown in figure 1. The two-dimensional NACA 0012 airfoil with a chord length of c is used as the profile of the self-propelled foil. All of the foils are arranged in tandem formation with an initial distance G_0. Each foil is driven by heaving and pitching motions, given by

$$h_i(t) = h_m \sin(2\pi ft + (i-1)\phi), \tag{2.1a}$$

$$\theta_i(t) = \theta_m \sin(2\pi ft - \pi/2 + (i-1)\phi), \tag{2.1b}$$

where $h_i(t)$ and $\theta_i(t)$ are respectively the instantaneous heaving and pitching motions of each foil, h_m is the heaving amplitude, θ_m is the pitching amplitude, f is the flapping frequency, ϕ is the phase difference between two adjacent foils, the script 'i' represents the serial number of each foil, and the pivot location of pitching motion is fixed at $c/3$.

The propulsion of each foil is controlled by Newton's second law, which can be described as follows (Deng & Caulfield 2018):

$$m\frac{\mathrm{d}^2X}{\mathrm{d}t^2} = F_x, \tag{2.2}$$

where X is the horizontal position of the foil and F_x is the horizontal component of the hydrodynamic force applied on the foil surface, which results from the hydrodynamic interactions. $m = \rho_s s$ is the mass of the foil, where ρ_s and s are respectively the density and area of the foil. In this study, the mass ratio is $\overline{m} = m/m_f = 1.0$, where $m_f = \rho s$ is the flow mass with equivalent area and ρ is the density of the fluid. The propelled direction is defined along the negative x direction. Thus, the instantaneous speed of each foil can be calculated as $u_i(t) = -\mathrm{d}X/\mathrm{d}t$. It should be pointed out that each foil is free only in the x direction, and is restrained in the y direction. Since only the cruising motion of fish schools and bird flocks has been considered here, the yaw motion can be neglected. Such a simplified model has also been adopted in some previous studies (Zhu *et al.* 2014; Becker *et al.* 2015; Ramananarivo *et al.* 2016; Peng *et al.* 2018*a*; Newbolt *et al.* 2019).

Three important indicators for quantifying the propulsive performance – the cycle-averaged propulsive speed, the cycle-averaged power consumption and the propulsive efficiency – are respectively calculated as

$$\overline{u}_i = \frac{1}{T}\int_0^T u_i(t)\mathrm{d}t, \quad \overline{P}_i = \frac{1}{T}\int_0^T \left(F_{iy}\frac{\mathrm{d}h_i(t)}{\mathrm{d}t} + M_i\frac{\theta_i(t)}{\mathrm{d}t}\right)\mathrm{d}t, \quad \overline{\eta} = \frac{\sum_{i=1}^{N}\overline{E}_{ik}}{\sum_{i=1}^{N}(\overline{P}_i T)}, \tag{2.3a–c}$$

where T is the flapping period. In the stable formation, all of the foils have the same cycle-averaged speed (i.e. $\overline{u} = \overline{u}_i$). F_{iy} and M_i are respectively the vertical force and torque applied on the ith foil surface. $\overline{E}_{ik} = 1/T\int_0^T \frac{1}{2}mu_i(t)^2\mathrm{d}t$ is the cycle-averaged kinetic energy of the ith foil.

The two-dimensional incompressible viscous flow over the multiple foils is governed by the Navier–Stokes equations

$$\frac{\partial \rho}{\partial t} + \boldsymbol{\nabla}\cdot(\rho\boldsymbol{v}) = 0, \tag{2.4a}$$

$$\frac{\partial \rho\boldsymbol{v}}{\partial t} + \boldsymbol{\nabla}\cdot(\rho\boldsymbol{v}\boldsymbol{v}^{\mathrm{T}} + p\boldsymbol{I}) = \nu\boldsymbol{\nabla}\cdot[\boldsymbol{\nabla}(\rho\boldsymbol{v}) + \boldsymbol{\nabla}(\rho\boldsymbol{v})^{\mathrm{T}}], \tag{2.4b}$$

where $\boldsymbol{v}$ is the flow velocity vector, p is the pressure, ν is the kinematic viscosity of flow and $\boldsymbol{I}$ is the unit tensor. The Reynolds number is defined as $Re = Uc/\nu$, where $U = 2\pi f h_m$ is the reference velocity. The Navier–Stokes equation is solved by using a simplified circular-function-based gas kinetic method (Yang *et al.* 2017*a*), while the interaction between the flapping foil and the surrounding flow is solved by using the velocity-correction-based immersed boundary method (Wu & Shu 2009). The numerical method has approximately second-order convergence accuracy, and the corresponding code has been validated for flapping foil simulations over a wide range of kinematics (Yang *et al.* 2017*b*; Lin, Wu & Zhang 2019*a*; Lin *et al.* 2019*b*).

Parameters	Values
Reynolds number, Re	200
Mass ratio, $\overline{m}$	1.0
Heaving amplitude, h_m/c	0.4
Flapping frequency, f	0.3
Pitching amplitude, θ_m	$\pi/9$
Initial distance, G_0/c	0.25, 0.5, 0.75, 1.0, 1.25, 1.5, 2.0, 2.5
Phase difference, ϕ	1.3π–1.8π ($\Delta = 0.1\pi$)
Number of foils, N	5, 10, 15

TABLE 1. Values of the controlled parameters used in the current simulations.

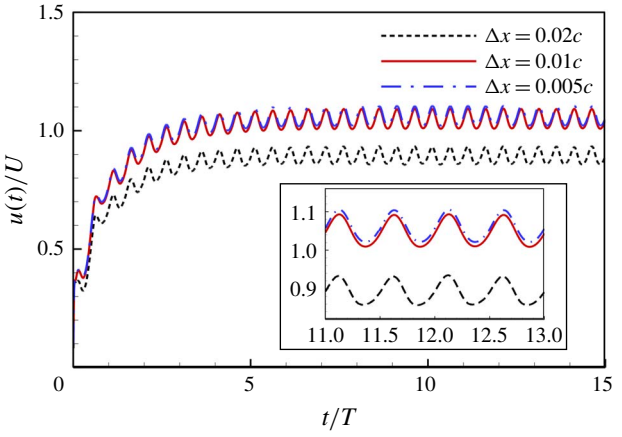

FIGURE 2. Time histories of the propulsive velocity of a single flapping foil obtained with different mesh spacings. The flapping parameters are $f = 0.3$, $h_m = 0.4c$, $\theta = \pi/9$ and $Re = 200$.

The controlled parameters used in the present work are listed in table 1. The current simulations are carried out on a rectangular computational domain of $100c \times 20c$, in which a region of $90c \times 10c$ is discretized by the uniform mesh. The foil surface is represented by 204 Lagrangian points with a uniform distribution. A no-slip boundary condition is imposed on the foil surface and a Dirichlet boundary condition is applied on the boundaries of the computational domain. First, a sensitivity test was carried out, as shown in figure 2, in which the propulsive velocity obtained from a mesh with $\Delta x = 0.01c$ is very close to that obtained from a mesh with $\Delta x = 0.005c$ (the difference of the cycle-averaged velocity is approximately 1.1 %). To strike a balance between the computational expense and accuracy that are related to the mesh, a grid of $\Delta x = 0.01c$ is chosen for the current simulations. In this study, it is assumed that a stable formation is reached when the horizontal separation distance between adjacent foils varies periodically. For example, figure 3(a) illustrates the time history of each separation distance in the case of $N = 5$, $\phi = 1.6\pi$ and $G_0/c = 0.25$. It is clear that the variation of each separation distance becomes periodic after approximately five periods; namely, a stable formation has been formed after five periods. In the current study, to make sure that a stable formation can be achieved, more than fifteen periods are completed for each case.

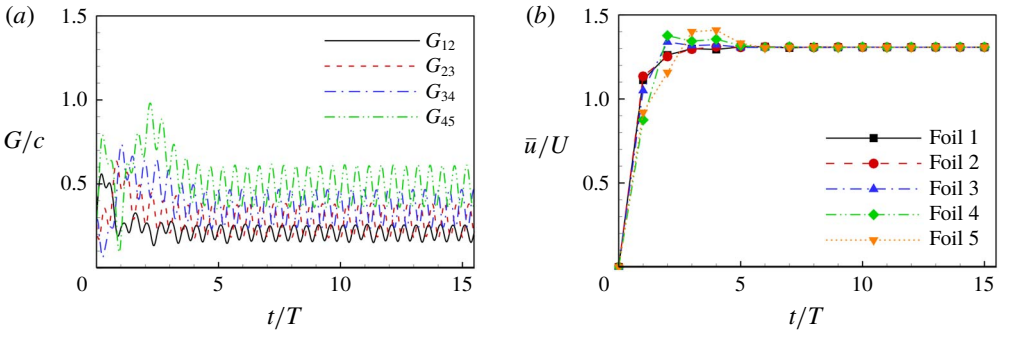

FIGURE 3. Time histories of (*a*) the separation distances between adjacent foils and (*b*) the mean speed of each foil in the case of $N = 5$, $\phi = 1.6\pi$ and $G_0/c = 0.25$. $G_{i,i+1}(i = 1, 2, \ldots, N-1)$ in (*a*) represents the horizontal distance between adjacent foils.

3. Results and discussion

First, the performance of five-foil system is studied. It is interesting that the compact formation can be spontaneously formed by multiple flapping foils via flow-mediated interactions. As shown in figure 3(*a*), the separation distances between adjacent foils vary drastically during the time period 0–5T. This is because the following foils encounter vortices shed from the leading foils. The vortex–body interactions generate repulsive and attractive forces on the following foils (Zhu *et al.* 2014). Consequently, the following foils undergo deceleration and acceleration processes during the time period 0–5T, as shown in figure 3(*b*). After several periods (in this case five periods), thanks to flow-mediated interactions, all of the foils can achieve the same cycle-averaged speed. As a consequence, each separation distance varies periodically; namely, a compact formation has been spontaneously formed. In the compact formation, these asynchronous flapping foils behave like a complete anguilliform undulated swimmer, as shown in figure 4(*a*). Consequently, this performance is called anguilliform-like swimming behaviour. One noteworthy feature of anguilliform-like swimming behaviour is that the separation distance between two adjacent foils is much smaller than 1.0c. Moreover, the reversed von Kármán vortex street is observed only behind the last foil. For more details about the anguilliform-like swimming behaviour, please refer to supplementary movie 1 available at https://doi.org/10.1017/jfm.2019.954.

This anguilliform-like swimming behaviour is not an isolated case for multiple self-propelled foils. It can be observed over a wide range of parameters, including the number of foils (N), the phase difference (ϕ), the initial distance (G_0) and the flapping amplitude (h_m and θ_m). Surprisingly, as the number of foils increases, anguilliform-like swimming behaviour still can be observed – such as for ten and fifteen foils considered in the current work, as shown in figure 4(*b*,*c*) and supplementary movies 2–3.

In addition, the effects of the phase difference and initial distance on the emergence of anguilliform-like swimming behaviour have been studied. The five-body system is selected, and other parameters are fixed as $f = 0.3$, $h_m/c = 0.4$, $\theta_m = \pi/9$. As shown in figure 5(*a*), anguilliform-like swimming behaviour can be observed for the five-body system when $1.4\pi \leqslant \phi \leqslant 1.7\pi$ and $G_0 \leqslant 1.5c$ (the grey region), and in these ranges the case which has the smaller phase difference can self-organize

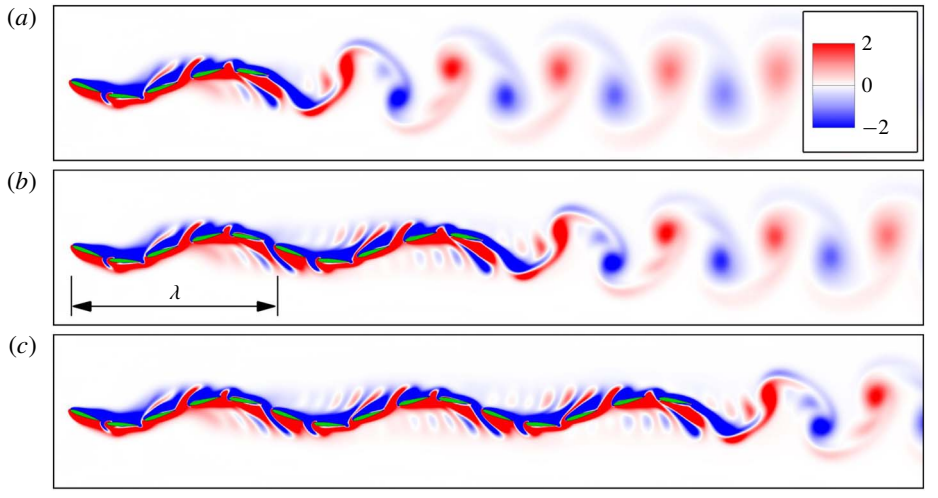

FIGURE 4. Instantaneous vorticity of multiple foils in anguilliform-like swimming behaviour at $t/T = 17$, in which the number of foils is $N =$ (*a*) 5, (*b*) 10, (*c*) 15; the corresponding parameters are $\phi = 1.6\pi$ and $G_0 = 0.25c$. For more details, please refer to supplementary movies 1–3.

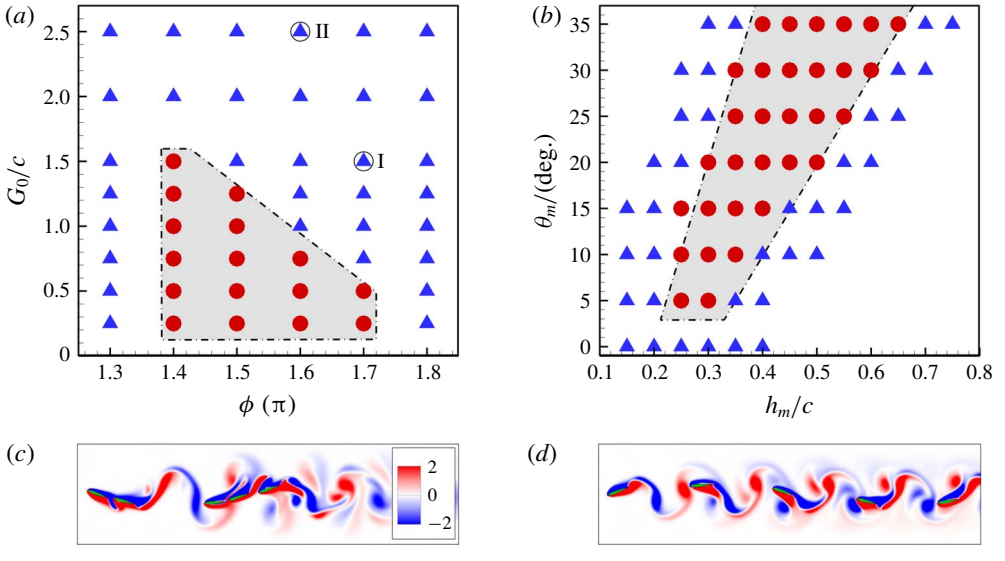

FIGURE 5. Parameter ranges of (*a*) $\phi - G_0$ and (*b*) $h_m - \theta_m$ in which the compact formation can be observed. Red circular symbols represent the compact formation and blue triangular symbols represent the sparse formation. Panels (*c*) and (*d*) illustrate the instantaneous vorticity of five foils in the sparse formation at (*c*) $t/T = 15.05$ and (*d*) $t/T = 15.5$, which respectively correspond to cases I and II in (*a*).

anguilliform-like swimming with a relatively larger initial distance. It means that the phase difference is crucial for the emergence of anguilliform-like swimming behaviour. On the other hand, in order to study the effect of the flapping amplitude on the emergence of anguilliform-like swimming behaviour, cases of $\phi = 1.6\pi$ and

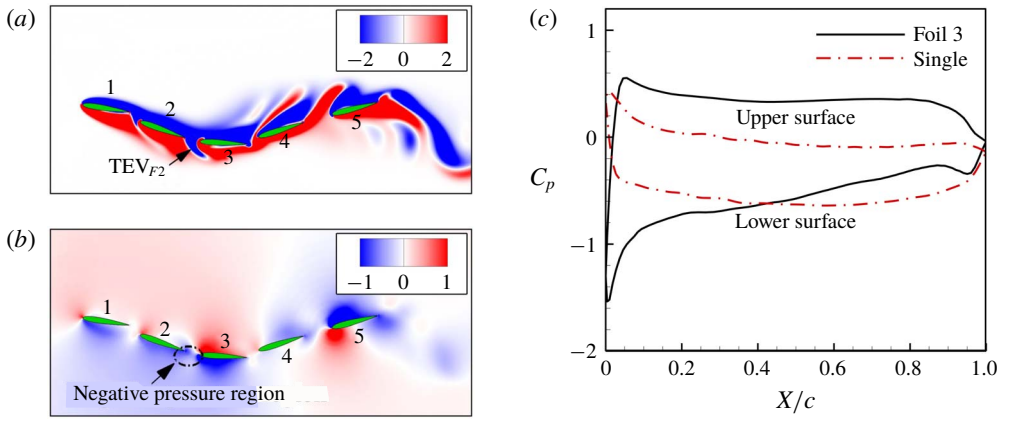

FIGURE 6. (*a*) Instantaneous vorticity and (*b*) pressure coefficient contours of the five-foil system in anguilliform-like swimming behaviour at time $t/T = 15.2$. (*c*) Instantaneous pressure coefficient distribution along the surfaces of foil 3 at time $t/T = 15.2$.

$G_0 = 0.25c$ with different heaving and pitching amplitudes have been simulated. As expected, anguilliform-like swimming behaviour can still be observed when the heaving and pitching amplitudes are appropriate, as shown in the grey region of figure 5(*b*). In particular, it is noted that anguilliform-like swimming can be observed over a wider range of h_m when θ_m increases. Moreover, it should be pointed out that the cycle-averaged speed of the anguilliform collective varies with the flapping amplitude. For example, in the case of $\theta_m = 35°$, the cycle-averaged speed of the anguilliform collective decreases as h_m/c increases from 0.4 to 0.65. Therefore, it implies that the flapping amplitude can influence the performance of the anguilliform collective. When the parameters are outside the grey region in figures 5(*a*) or 5(*b*), the sparse formation can be observed, in which at least one foil is far away from its leader, as shown in figure 5(*c*,*d*). The sparse formation is similar to the observation in the work of Peng *et al.* (2018*b*).

For multiple foils ($N = 5$–15) in the current work, maintenance of the compact formation may be related to the appropriate phase difference ($\phi = 1.4\pi$–1.7π), which allows the following foil to easily capture the trailing edge vortex (TEV) of the leading foil. As shown in figure 4 and supplementary movies 1–3, it is clear that the vertical distance between the trailing edge of the leading foil and the leading edge of the following foil is small. Such a small vertical distance allows the following foil to easily capture the TEV of the leading foil. As shown in figure 6(*a*), for example, the TEV of foil 2 (i.e. TEV$_{F2}$) is captured by foil 3 before it is fully developed (such as at time $t/T = 15.2$ here). The captured TEV can induce a negative pressure region ahead of the following foil – as shown in figure 6(*b*,*c*), for example – which can generate a suction effect on the following foil. Moreover, similar TEV capturing can be observed for the other foils, as shown in supplementary movies 1–3. Consequently, the following foil can be attracted by the leading foil via the suction effect of the captured TEV, and the compact formation can be maintained for multiple foils. The captured TEV is like a spring connecting the adjacent foils.

In order to further analyse the performance of multiple foils in anguilliform-like swimming behaviour, the cycle-averaged propulsive speed, the cycle-averaged power consumption and the propulsive efficiency of multiple foils are calculated. Figure 7

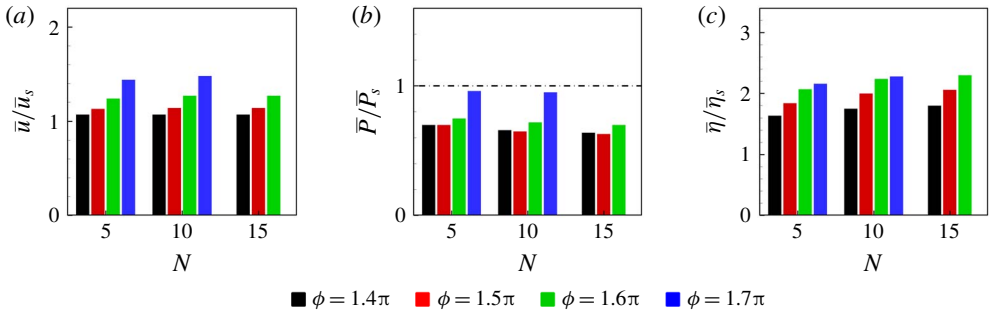

FIGURE 7. Ratios of cycle-averaged (*a*) propulsive speed, (*b*) power consumption and (*c*) propulsive efficiency of the anguilliform collective to those of the isolated foil. The subscript '*s*' denotes the single foil.

shows the ratios of the cycle-averaged propulsive speed, the cycle-averaged power consumption and the propulsive efficiency of the anguilliform collective to those of the isolated foil. For comparison, the cycle-averaged power consumption of the anguilliform collective is calculated as the mean value of each foil – i.e. $\overline{P} = 1/N \sum_{i=1}^{N} \overline{P}_i$. Note that the data for the fifteen-foil system with $\phi = 1.7\pi$ are absent, since the fifteen-foil system in the case of $\phi = 1.7\pi$ and $G_0 = 0.25c$ is unable to achieve the compact formation, it means that the number of foils which can be adopted for the anguilliform-like swimming behaviour is finite.

It can be seen from figure 7(*a*) that the cycle-averaged speed of the anguilliform collective is obviously larger than that of the isolated foil. Moreover, it should be pointed out the propulsive velocity increases slightly as the number of foils increases from $N = 5$ to $N = 10$, and keeps unchanged as the number of foils further increases ($N = 15$). It seems to indicate that there is a threshold number of foils above which the speed of the anguilliform collective is unchanged (the threshold value is approximately $N = 5$ in the present work). On the other hand, it is clear that the swimming speed of the anguilliform collective increases with increasing phase difference. Such a variation of speed induced by the phase difference can be explained by the variation of the anguilliform-like swimming wavelength, which can be described as follows.

Here the anguilliform-like swimming wavelength is defined as the horizontal distance between the leading edges of two adjacent foils whose flapping motions are the same as each other, as illustrated in figure 4(*b*). Thus, it can be calculated as $\lambda = (2\pi \,|\, X_1 - X_N \,|)/((N-1)(2\pi - \phi))$, where X_1 and X_N are, respectively, the horizontal positions of the first and last foils. The ten-foil system ($N = 10$) is used to calculate the wavelength, since at least one complete wave can be observed in the anguilliform-like swimming of ten foils. As a result, the values of swimming wavelength in the cases $\phi = 1.4\pi$, 1.5π, 1.6π and 1.7π, respectively, are $\lambda = 5.08c$, $5.65c$, $6.71c$ and $8.89c$. Namely, the swimming wavelength of the anguilliform collective is increased as the phase difference increases. Since the undulated swimming speed increases with increasing wavelength (Liao 2002; Liu & Curet 2018), the swimming speed of the anguilliform collective increases with the phase difference.

On the other hand, it is clear that the power consumption of the anguilliform collective is lower than that of the isolated foil, as illustrated in figure 7(*b*). Consequently, the propulsive efficiency of the anguilliform collective is larger than

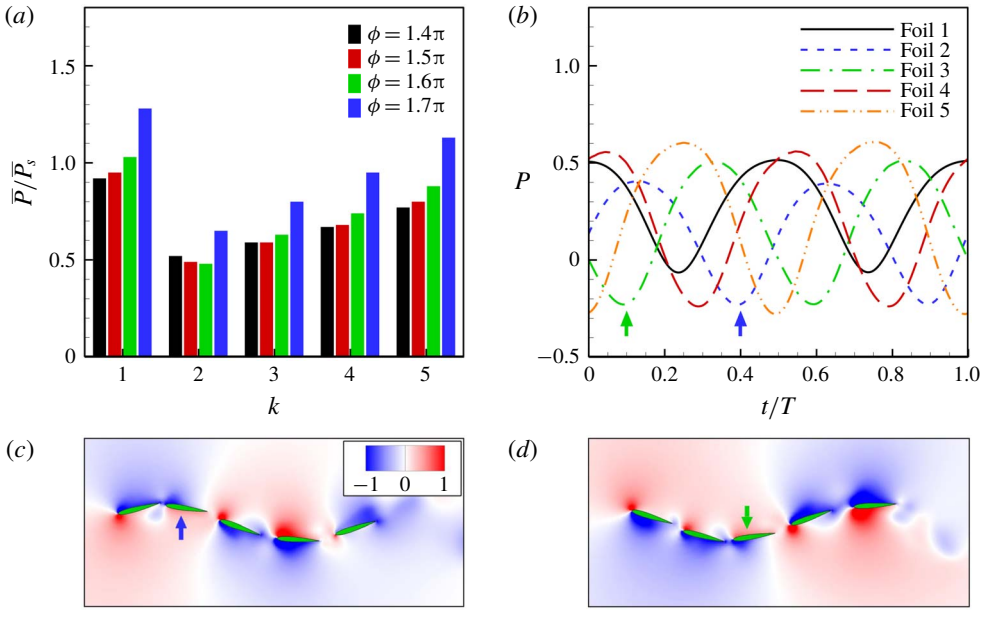

FIGURE 8. (*a*) Cycle-averaged power consumption and (*b*) time histories of power consumption of five foils ($\phi = 1.6\pi$) in anguilliform-like swimming behaviour. The instantaneous pressure distribution at time (*c*) $t/T = 0.4$ and (*d*) $t/T = 0.1$. The horizontal axis '*k*' in (*a*) denotes the serial number of each foil.

that of the isolated foil, as shown in figure 7(*c*). Furthermore, the energy consumption is decreased as the number of foils increases, but it increases with increasing phase difference. However, the propulsive efficiency increases with increasing phase difference and the number of foils. As a consequence, multiple foils in the compact formation have a greater velocity, lower power consumption and a higher propulsive efficiency, as compared with the isolated foil.

In order to further investigate the energetic advantage of multiple foils in anguilliform-like swimming behaviour, the power consumption of each foil is calculated, as shown in figure 8(*a*). It can be seen that the foils in the middle positions of the compact formation have significant energy savings – such as foils 2–3 for example. This is because the middle foil has a significant power extraction process when it moves near the peaks of flapping motion, as shown in figure 8(*b*). As shown in figure 8(*c*,*d*), the blue and green arrows respectively represent the flapping directions of foils 2–3 at the moments which are indicated by the corresponding arrows in figure 8(*b*). It is clear that, according to the flapping direction, both foils 2 and 3 have positive pressure at the leeward surface and negative pressure at the windward surface. Such a pressure distribution can generate a lift whose direction is the same as the flapping direction; thus, the foil can harvest energy from the surrounding flow (Kinsey & Dumas 2008). In addition, energy extraction has been observed for the other foils which are in the middle positions of the compact formation, no matter whether the phase difference or the number of foils changes. Consequently, the energy saving of multiple-foil system in the compact formation results primarily from the power extraction of the middle foils, and increases as the number of foils increases.

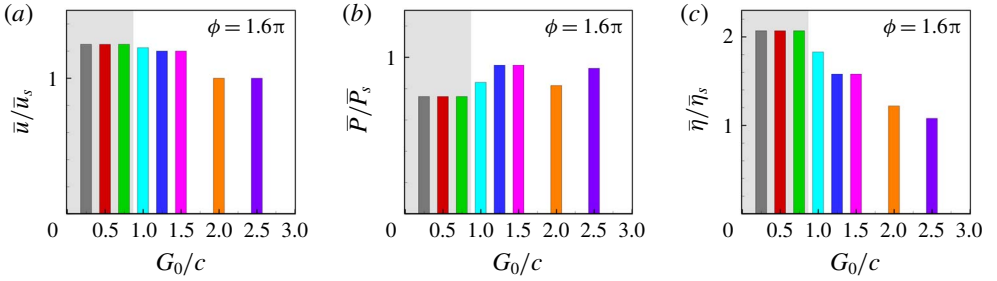

FIGURE 9. Ratio of cycle-averaged (*a*) propulsive speed, (*b*) power consumption and (*c*) propulsive efficiency of the five-foil system at different initial distances relative to those of the isolated foil. The grey region represents the compact formation and the remaining white region is the sparse formation.

Moreover, to further compare the performance of multiple foils in different formations, the case of a five-foil system with $\phi = 1.6\pi$ is selected. As shown in figure 9, the cycle-averaged propulsive speed, the cycle-averaged power consumption and the propulsive efficiency of the five-foil system at different initial distances are calculated. It is clear that multiple foils in the compact formation (the grey region) can produce higher speed, lower power consumption and higher propulsive efficiency than they can in the sparse formation. Consequently, the compact formation is a better recommendation than the sparse formation for multiple foils. On the other hand, it can be seen that the performance of a multiple-foil system varies significantly with the initial distance in the sparse formation. This is caused by the generation of different types of sparse formation, as shown for example in figure 5(*b*,*c*). However, the multiple-foil system in the sparse formation still has a higher efficiency than the isolated foil. It means that flow-mediated interactions have only constructive effects on the performance of multiple foils. This is different from the results reported in previous studies (Akhtar *et al.* 2004; Rival *et al.* 2011; Broering *et al.* 2012; Boschitsch *et al.* 2014), in which both constructive and destructive hydrodynamic effects on the performance of tethered tandem individuals have been observed. The reason why the destructive hydrodynamic effect disappears here may be that self-propelled bodies can avoid destructive flow-mediated interactions by adjusting their positions appropriately.

4. Conclusions

In summary, the performance of multiple self-propelled foils in tandem formation, whose flapping motions are asynchronous with a phase difference, is studied in the current work. The results achieved indicate that the compact formation can be spontaneously formed by multiple foils via flow-mediated interactions. In the compact formation, all of the foils are close to each other and perform like a complete anguilliform undulated swimmer. Moreover, such anguilliform-like swimming behaviour can be observed over a wide range of parameters, including the number of foils, the phase difference, the initial distance, the heaving amplitude and the pitching amplitude. The appropriate phase difference is crucial to maintain the compact formation of multiple foils.

In the anguilliform-like swimming behaviour, both velocity enhancement and energy saving can be achieved by the multiple-foil system, as compared with the isolated

foil. In addition, the velocity enhancement increases with increasing phase difference. Furthermore, the energy benefit results primarily from the power extraction of the middle foils, and is increased as the number of foils increases. On the other hand, the multiple-foil system in the compact formation always outperforms that in the sparse formation. As a consequence, the compact formation may be an optimal strategy for multiple self-propelled foils, and it can be self-organized by controlling the phase difference and the initial distance between adjacent individuals.

Finally, it should be pointed out that, in this study, the lateral motion of foils is restrained, and only the propulsion in the stationary fluid is considered. In fact, real fish schools and bird flocks are free to move in multiple directions, and they often travel in the wake behind objects. Consequently, some different phenomena may be observed if lateral motion or altered flow is considered. For example, a stable movement arrangement may not be formed if there is a lateral force on the foil. Thus, analysis of the stability of flapping foils should also be performed. These situations will be considered in future work.

Acknowledgements

J.W. acknowledges the support of the National Natural Science Foundation of China (grant no. 11622219) and the Fundamental Research Funds for the Central Universities (grant no. NE2017102). X.L. acknowledges the support of the Funding for Outstanding Doctoral Dissertation in NUAA (grant no. BCXJ19-02) and Postgraduate Research & Practice Innovation Program of Jiangsu Province (grant no. KYCX19_0154). This work is also supported by the Priority Academic Program Development of Jiangsu Higher Education Institutions (PAPD).

Declaration of interests

The authors report no conflict of interest.

Supplementary movies

Supplementary movies are available at https://doi.org/10.1017/jfm.2019.954.

References

AKHTAR, I., MITTAL, R., LAUDER, G. V. & DRUCKER, E. 2004 Hydrodynamics of biologically inspired tandem flapping foil configuration. *Theor. Comput. Fluid Dyn.* **21**, 155–170.

ASHRAF, I., BRADSHAW, H., HA, T. T., HALLOY, J., GODOY-DIANA, R. & THIRIA, B. 2017 Simple phalanx pattern leads to energy saving in cohesive fish schooling. *Proc. Natl Acad. Sci. USA* **114**, 9599–9604.

ASHRAF, I., GODOY-DIANA, R., HALLOY, J., COLLIGNON, B. & THIRIA, B. 2016 Synchronization and collective swimming patterns in fish (*Hemigrammus bleheri*). *J. R. Soc. Interface* **13**, 20160734.

BECKER, A. D., MASOUD, H., NEWBOLT, J. W., SHELLEY, M. & RISTROPH, L. 2015 Hydrodynamic schooling of flapping swimmers. *Nat. Commun.* **6**, 8514.

BOSCHITSCH, B. M., DEWEY, P. A. & SMITS, A. J. 2014 Propulsive performance of unsteady tandem hydrofoils in an in-line configuration. *Phys. Fluids* **26**, 051901.

BROERING, T. M., LIAN, Y. S. & HENSHAW, W. 2012 Numerical investigation of energy extraction in a tandem flapping wing configuration. *AIAA J.* **50**, 2295–2307.

COUZIN, I. D. 2009 Collective cognition in animal groups. *Trends Cognit. Sci.* **13**, 36–43.

DENG, J. & CAULFIELD, C. P. 2018 Horizontal locomotion of a vertically flapping oblate spheroid. *J. Fluid Mech.* **840**, 688–708.

DONG, G.-J. & LU, X.-Y. 2007 Characteristics of flow over traveling wavy foils in a side-by-side arrangement. *Phys. Fluids* **19**, 057107.

FILELLA, A., NADAL, F., SIRE, C., KANSO, E. & ELOY, C. 2018 Model of collective fish behavior with hydrodynamic interactions. *Phys. Rev. Lett.* **120**, 198101.

GAO, A. & TRIANTAFYLLOU, M. S. 2018 Independent caudal fin actuation enables high energy extraction and control in two-dimensional fish-like group swimming. *J. Fluid Mech.* **850**, 304–335.

GUAZZELLI, E. & HINCH, J. 2011 Fluctuations and instability in sedimentation. *Annu. Rev. Fluid Mech.* **43**, 97–116.

HEMELRIJK, C. K. & HILDENBRANDT, H. 2012 Schools of fish and flocks of birds: their shape and internal structure by self-organization. *Interface Focus* **2**, 726–737.

KIM, S., HUANG, W.-X. & SUNG, H. J. 2010 Constructive and destructive interaction modes between two tandem flexible flags in viscous flow. *J. Fluid Mech.* **661**, 511–521.

KINSEY, T. & DUMAS, G. 2008 Parametric study of an oscillating airfoil in a power extraction regime. *AIAA J.* **46**, 1318–1330.

KOCH, D. L. & SUBRAMANIAN, G. 2011 Collective hydrodynamics of swimming microorganisms: living fluids. *Annu. Rev. Fluid Mech.* **43**, 637–659.

KURT, M. & MOORED, K. W. 2018 Flow interactions of two- and three-dimensional networked bio-inspired control elements in an in-line arrangement. *Bioinspir. Biomim.* **13**, 045002.

LIAO, J. C. 2002 Swimming in needlefish (Belonidae): anguilliform locomotion with fins. *J. Exp. Biol.* **205**, 2875–2884.

LIN, X., WU, J. & ZHANG, T. 2019*a* Performance investigation of a self-propelled foil with combined oscillating motion in stationary fluid. *Ocean Engng* **175**, 33–49.

LIN, X., WU, J., ZHANG, T. & YANG, L. 2019*b* Phase difference effect on collective locomotion of two tandem autopropelled flapping foils. *Phys. Rev. Fluids* **4**, 054101.

LIU, H. & CURET, O. 2018 Swimming performance of a bio-inspired robotic vessel with undulating fin propulsion. *Bioinspir. Biomim.* **13**, 056006.

MAERTENS, A. P., GAO, A. & TRIANTAFYLLOU, M. S. 2017 Optimal undulatory swimming for a single fish-like body and for a pair of interacting swimmers. *J. Fluid Mech.* **813**, 301–345.

MARRAS, S., KILLEN, S. S., LINDSTROM, J., MCKENZIE, D. J., STEFFENSEN, J. F. & DOMENICI, P. 2015 Fish swimming in schools save energy regardless of their spatial position. *Behav. Ecol. Sociobiol.* **69**, 219–226.

MUSCUTT, L. E., WEYMOUTH, G. D. & GANAPATHISUBRAMANI, B. 2017 Performance augmentation mechanism of in-line tandem flapping foils. *J. Fluid Mech.* **827**, 484–505.

NEWBOLT, J. W., ZHANG, J. & RISTROPH, L. 2019 Flow interactions between uncoordinated flapping swimmers give rise to group cohesion. *Proc. Natl Acad. Sci. USA* **116**, 2419–2424.

PARTRIDGE, B. L. & PITCHER, T. J. 1979 Evidence against a hydrodynamic function for fish schools. *Nature* **279**, 418–419.

PENG, Z.-R., HUANG, H. & LU, X.-Y. 2018*a* Collective locomotion of two closely spaced self-propelled flapping plates. *J. Fluid Mech.* **849**, 1068–1095.

PENG, Z.-R., HUANG, H. & LU, X.-Y. 2018*b* Hydrodynamic schooling of multiple self-propelled flapping plates. *J. Fluid Mech.* **853**, 587–600.

PORTUGAL, S. J., HUBEL, T. Y., FRITZ, J., HEESE, S., TROBE, D., VOELKL, B., HAILES, S., WILSON, A. M. & USHERWOOD, J. R. 2014 Upwash exploitation and downwash avoidance by flap phasing in ibis formation flight. *Nature* **505**, 399–402.

RAMANANARIVO, S., FANG., F., OZA, A., ZHANG, J. & RISTROPH, L. 2016 Flow interactions lead to orderly formations of flapping wings in forward flight. *Phys. Rev. Fluids* **1**, 071201.

RIVAL, D., HASS, G. & TROPEA, C. 2011 Recovery of energy from leading- and trailing-edge vortices in tandem-airfoil configurations. *J. Aircraft* **48**, 203–211.

SHOELE, K. & ZHU, Q. 2015 Performance of synchronized fins in biomimetic propulsion. *Bioinspir. Biomim.* **10**, 026008.

SUMPTER, D. J. 2006 The principles of collective animal behavior. *Phil. Trans. R. Soc. Lond.* B **361**, 5–22.

UDDIN, E., HUANG, W.-X. & SUNG, H. J. 2015 Actively flapping tandem flexible flags in a viscous flow. *J. Fluid Mech.* **780**, 120–142.

USHERWOOD, J. R., STAVROU, M., LOWE, J. C., ROSKILLY, K. & WILSON, A. M. 2011 Flying in a flock comes at a cost in pigeons. *Nature* **474**, 494–497.

WEIHS, D. 1973 Hydromechanics of fish schooling. *Nature* **241**, 290–291.

WU, J. & SHU, C. 2009 Implicit velocity correction-based immersed boundary-lattice Boltzmann method and its applications. *J. Comput. Phys.* **228**, 1963–1979.

YANG, L. M., SHU, C., YANG, W. M. & WANG, Y. 2017*a* A simplified circular function-based gas kinetic scheme for simulation of incompressible flows. *Intl J. Numer. Meth. Fluids* **85**, 583–598.

YANG, L. M., SHU, C., YANG, W. M., WANG, Y. & WU, J. 2017*b* An immersed boundary-simplified sphere function-based gas kinetic scheme for simulation of 3D incompressible flows. *Phys. Fluids* **29**, 083605.

ZHU, X., HE, G. & ZHANG, X. 2014 Flow-mediated interactions between two self-propelled flapping filaments in tandem configuration. *Phys. Rev. Lett.* **113**, 238105.